UDC 616.89–008:612.825:616.079

M. HASHEMIAN[1,2] and H. POURGHASSEM[1,2]

DECISION-LEVEL FUSION-BASED STRUCTURE OF AUTISM DIAGNOSIS USING INTERPRETATION OF EEG SIGNALS RELATED TO FACIAL EXPRESSION MODES

Received May 22, 2015

A structure of decision-level fusion-based autism diagnosis using analysis of EEG signals related to presentation of facial expression modes has been proposed. EEG signals of autistic and normal children were recorded during processing images of emotional facial expression modes, such as sadness, happiness, and calmness. Then brain signals were mapped into the feature space by applying a novel hybrid model utilizing the brain potentials recorded during the examination task. The aim of mapping was to achieve separation of the autistic samples from normal ones with the highest precision. The created map provides the feature vectors that reflected spatial, temporal, and spectral data, as well as the coherence degrees for distinct areas of the brain. The mapping process was optimized using a genetic algorithm by assigning weighs to the feature vectors. Then the feature vectors corresponding to the three facial expressions of emotional modes were classified by support vector machines. Finally, using decision-level fusion through a majority voting rule, we see that the proposed structure is able to effectively distinguish the autistic individuals from normal ones.

KEYWORDS: autism spectrum disorders (ASDs), facial expression modes, EEG signal interpretations, hybrid model, decision-level fusion.

INTRODUCTION

Autism, Asperger's syndrome, pervasive developmental disorder (not otherwise specified as childhood disintegrative disorder), and Rett's syndrome are known as pervasive developmental disorders. The autism spectrum disorders (ASDs) refer to autism *per se*, Asperger's syndrome, and pervasive developmental disorder not otherwise specified [1]. Autism is a neurological disorder that hinders the brain from functioning properly in terms of social situations and communicative skills [1–3]. Three main cognitive theories have been proposed concerning the individuals with autism, such as the theory of mind deficit, executive dysfunction, and the theory of weak central coherence. With the help of these theories, the nature of behavioral functions of children with ASD can be accounted for to some extent. Recent reports and studies indicated that the prevalence rate of the mentioned disorder is still increasing in different nations [4–10]. The diagnosis of autism is not an easy process; it generally requires a set of certain behavioral and cognitive characteristics.

At present, researchers are trying to find ASD diagnostic approaches through electrophysiological and neuroimaging techniques. Among these methods, interpretation of EEG signals is one of the fundamental tools in diagnosing and identifying neurophysiological disorders. Since EEG signals contain extensive high-resolution temporal information, the respective analysis has significant advantages in comparison with that in computer imaging techniques [11, 12]. In addition, EEG is relatively easy to use and more economical as well. Therefore, researchers are inclined to analyze EEG signals of autistic individuals and to compare these signals with normal ones.

In simple terms, the researchers, using pattern recognition techniques, have succeeded in providing diagnostic algorithms with different performance [13], so that various feature extraction methods were evaluated to distinguish children with ASD based on EEG

[1] Digital Processing and Machine Vision Research Center, Najafabad Branch, Islamic Azad University, Najafabad, Iran.
[2] Department of Electrical Engineering, Najafabad Branch, Islamic Azad University, Najafabad, Iran.
Correspondence should be addressed to H. Pourghassem (e-mail: h_pourghasem@iaun.ac.ir).

signals. For example, Sheikhani et al. [14] utilized Lempel-Ziv (LZ) complexity, short-time Fourier transform (STFT), and STFT at a bandwidth (STFT-BW) in the total spectrum. Further, Behnam et al. [15] calculated the STFT-BW component in the alpha frequency range (8–12 Hz) as a feature. Then, Higuchi's fractal (FD) and Katz's fractal dimensions were computed in all EEG sub-bands and in the entire spectrum [12]. Moreover, Razali et al. [16] examined the Gaussian mixture model as a method of feature extraction for analyzing brain signals in the frequency domain. In another work, Bosl et al. [17] used modified multiscale entropy (MMSE) as a feature vector. Later on, a few authors [18] applied principal components analysis (PCA) to STFT of the EEG signals. Also, Duffy et al. [19] employed PCA of the coherence data as an objective technique to meaningfully reduce the number of variables.

Our study proposes a diagnostic algorithm based on a hybrid model. This means that this algorithm classifies EEG signals of children with autism and differentiates these signals from normal ones during perception of images of the facial expression modes. In this hybrid model, brain signals are mapped into a feature space by utilizing brain potentials related to certain emotional modes. In this algorithm, EEG signals of autistic and normal children are recorded during processing three different emotional facial expressions (sadness, happiness, and calmness); after preprocessing them, a vector-space map is written by means of the proposed hybrid model. The created map provides the feature vectors reflecting the spatial, temporal, and spectral data, as well as the coherence degrees for the distinct brain areas. The mapping process is optimized by a genetic algorithm by assigning weights to the feature vectors. Then, the feature vectors corresponding to the three facial expressions of emotional modes are classified by Support Vector Machines (SVMs). Finally, using decision-level fusion through the majority voting rule, we see that the proposed algorithm helps to distinguish effectively autistic and normal children from each other.

METHODS

Participants. Six children (four boys and two girls) ranging in age from 7 to 9 years were diagnosed as autistic by the Autistic Society of Malaysia according to the DSM-IV criteria. An intelligence quotient measure of the autistic children was determined based on the Stanford Binet test. The IQ test took about 2–3 days to be completed. In this test, the IQ levels are categorized into very gifted or highly advanced (VG), superior (Su), high average (HA), borderly impaired or delayed (BI), moderately impaired or delayed (Mo), gifted or very advanced (G), average (Ave), low average (LA), and mildly impaired or delayed (MI). We considered ASD children with either Ave or LA in their verbal or nonverbal IQs. The control group consisted of six boys, 7 to 9 years old, without a history of neurologic treatment. Each of the children in the non-ASD group took about 3–4 h (continuous session) to complete the IQ test. The normal group had an average level in both verbal and nonverbal IQs.

Stimuli. The stimuli consisted of visual presentation of images of sad, happy, and calm human faces, which were shown as movie clips with a duration of 1 min for each affective state. Each face was shown for only 8 sec; there was a 2-sec-long time interval after displaying each face to let the child change his/her mood to watch the next face.

EEG Recording. The participants were asked to sit in a light and quiet room, and electrodes were placed on their heads according to the international 10–20-system. The channels C3, C4, F3, F4, P3, P4, T3, and T4 were used, and CZ was considered as reference. While the participants were watching the video clips of sad, happy, and calm human faces, their EEGs were recorded using the BIMEC EEG set (Germany). The recorded EEG signals are then saved for off-line processing. The channel data were sampled with a 250 sec^{-1} frequency and filtered with low-pass elliptic filters in the frequency range 0–64 Hz. Elliptical filters effectively attenuate unwanted frequency-band effects. To remove the impact of artifacts of the 50 Hz electricity network, a notch filter was used.

Structure of the Proposed Decision-Level Fusion-Based Autism Diagnosis. The proposed algorithm consists of four major steps of feature extraction, mapping to the feature space, optimization of this mapping through the weight assignment, classification of the feature vectors, and data fusion in the decision level (a decision-making phase). Figure 1 shows a block diagram of our proposed decision-level fusion-based autism diagnosis structure. These stages are completely described below.

Feature Extraction. There are important data in EEG signals that help us to effectively distinguish between autistic and normal children. In order to extract this valuable information, a hybrid model

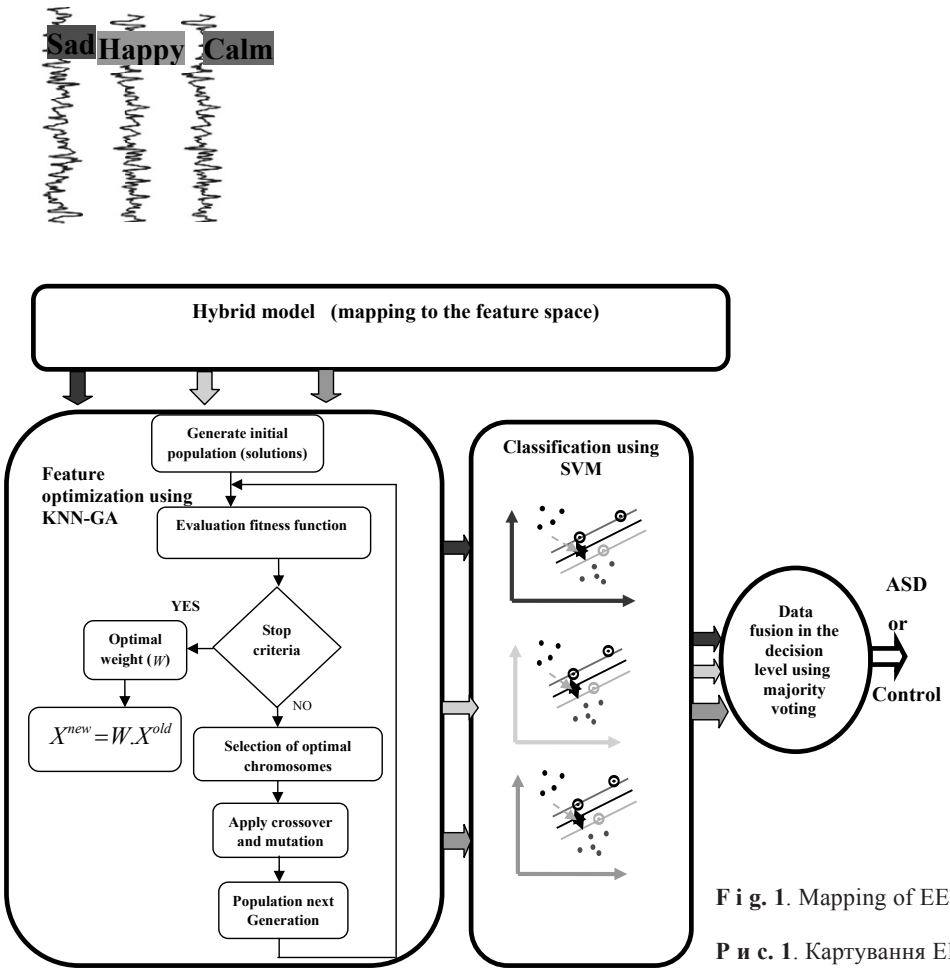

F i g. 1. Mapping of EEG signals to the feature space.

Р и с. 1. Картування ЕЕГ-сигналів у просторі ознак.

based on the EEG signals has been provided. In this step, the signals are mapped in a vector space. In a sense, the feature vectors are produced through this model (Fig. 2). The merits of our proposed hybrid model include (i) nearly all of the brain potentials occurring during the examination task employed; (ii) it was organized based on utilizing distinct characteristics between the two groups, and (iii) no dimension reduction algorithms were used. As a result, no valuable data were lost. In this model, EEG signals are divided into l-sec-long epochs. Then a number of features are extracted based on a hybrid model. Here, the nature of extracted features from EEG signals is described, and then the structure of the hybrid model is discussed.

Discrete Fourier Transform (MDFT) Coefficients. The EEG signals in each epoch can be considered as a time series. The MDFT in a time series is defined as follows [20, 21]:

$$MDFT = \frac{\sum_{n=1}^{N} X_k}{N}, \quad (1)$$

$$X_k = \sum_{n=0}^{N-1} x_n e^{-j2\pi kn/N}, \quad (2)$$

where x_n is the nth sample, and N is the total number of samples in each epoch.

Log Energy in the δ, θ, α, β, and γ Bands. Due to the nonstationary nature of EEG signals, these signals should be decomposed into frequency bands; hence, a time-frequency transform (such as wavelet transform) is an appropriate tool to extract the features [22]. Wavelet transform is the product of the correlation between the frequency content of the signal and a mother wavelet function at different scales [23, 24]. Accordingly, the continuous wavelet transform can be defined by the following formula:

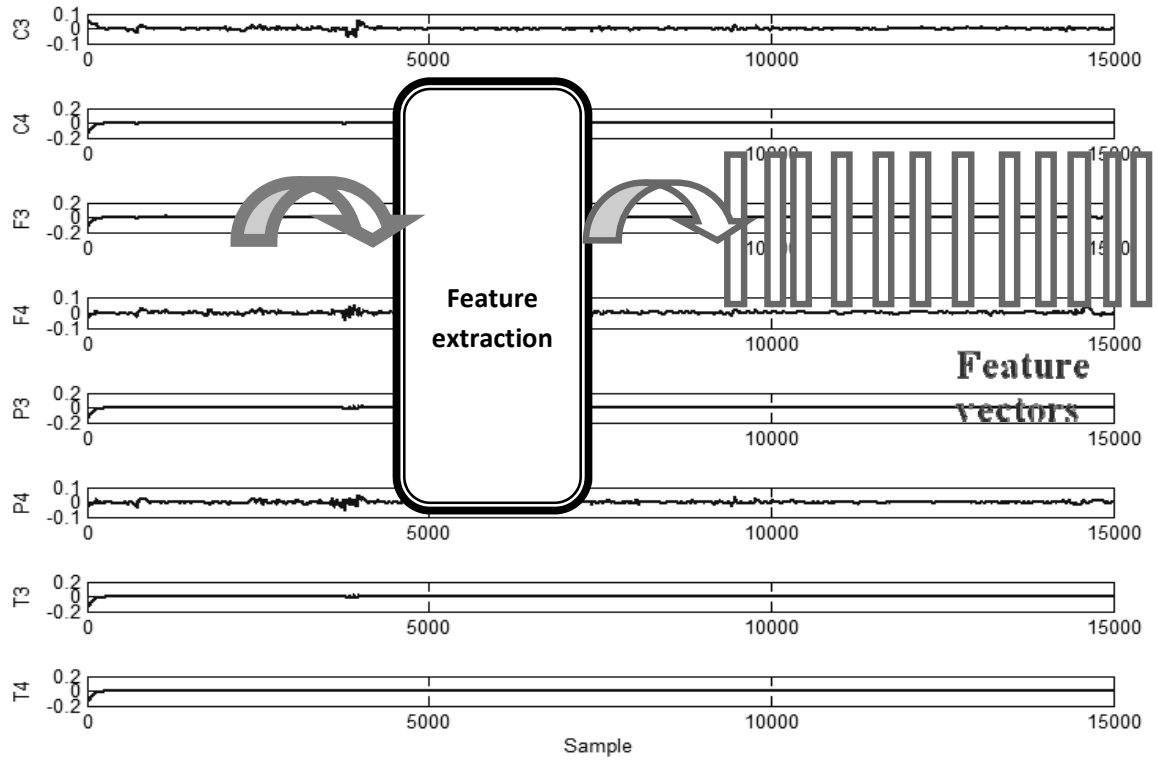

F i g. 2. Block diagram of wavelet decomposition of EEG into frequency bands.

Р и с. 2. Блок-діаграма wavelet-декомпозиції ЕЕГ у частотні смуги.

$$CWT_X^{\psi}(\tau,s) = \Psi_X^{\psi}(\tau,s) = \frac{1}{\sqrt{|s|}}\int_{-\infty}^{+\infty} x(t)\Psi^*(\frac{t-\tau}{s})dt, \quad (3)$$

where $x(t)$ is the signal to be analyzed, and $\Psi(t)$ is called the mother wavelet; * denotes the complex conjugate, s is the scale variable ($s \neq 0$)), and τ is the time shift variable. In this study, band-limited EEG signals (0–64 Hz) were decomposed into five bands, gamma (32–64 Hz), beta (16–32 Hz), alpha (8–16 Hz), theta (4–8 Hz), and delta (0–4 Hz), by analyzing the wavelet at four levels (scales) with Daubechies 4 [25]. Figure 3 shows a block diagram of this decomposition.

Log Energy Beta/Alpha Ratio. The ratio of beta and alpha brain waves [26] is a criterion of the arousal magnitude. The brain signals are recorded during emotional facial expression processing; this is why extraction of this feature from EEG signals can be a useful tool in distinguishing between autistic and normal children.

Mean of the Squared Magnitude of Coherence (MSMC). The coherence measures the coupling between two distinct time series in the frequency domain. The resulting coherence value will allow one to show close relations between two brain areas [27]. In our study, the coherence degree between the left and right hemispheres of the brain was calculated; the coherence degree within one single hemisphere was not examined. Due to the four channels of recording from each hemisphere, the respective values are very close to each other [28]. Therefore, calculation of coherence between the close channels is not permissible. Hence, the samples of channels were filtered in the range 0–0.64 Hz. The MSMC was calculated in the same frequency range with a resolution of 1.0 Hz as

$$MSMC = \sum_{f=0}^{64} c_{xy}(f), \quad (4)$$

where C_{xy} is defined as

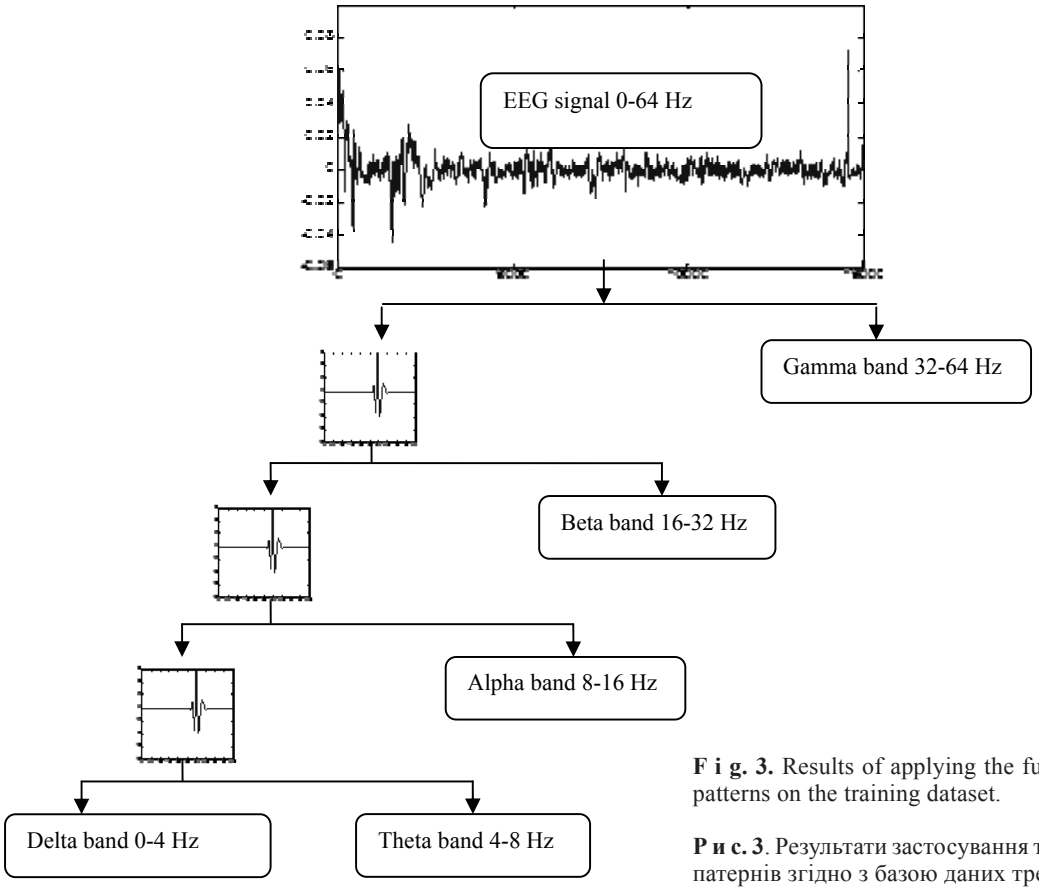

F i g. 3. Results of applying the fusion methods in diagnosing the patterns on the training dataset.

Р и с. 3. Результати застосування техніки злиття для діагностики патернів згідно з базою даних тренування.

$$C_{xy}(f) = \left| \frac{p_{xy}(f)}{(p_{xx}(f)p_{yy}(f))^{\frac{1}{2}}} \right|, \qquad (5)$$

where $p_{xx}(f)$ and $p_{yy}(f)$ are the power spectral densities of the channels x and y, respectively. Also, $p_{xy}(f)$ represents the cross power spectral density of the channels x and y.

Hybrid Model. So far, the nature of features used in the model was introduced. It is important how these features must be arranged and how the channel epochs must be incorporated to produce useful information. In simple terms, by using all the channel samples, this model is capable of representing simultaneously the feature vectors in any given time; the vectors include the place, time, and spectral information. To construct the hybrid model, we performed the following steps:

(i) Segmentation of all the channel samples into l-sec-long epochs (W is the number of epochs).

(ii) Receiving of the nth epoch of all channels (n=1:W)

(a) MDFT calculation.

(b) Calculation of the Log energy beta/ alpha ratio.

(c) MSMC calculation between the channels of the left and right hemispheres.

(d) Calculation of the Log energy in sub-bands δ, θ, α, β, and γ for the total sample resulting from all epoch channels.

(iii) Repetition of step 2 until $n \leq W$.

Finally, this algorithm yields a $d \times W$ matrix for an EEG signal where W signifies the number of epochs and d denotes the number of extracted features.

Weight Assignment using a K-nearest Neighbors Genetic Algorhythm (KNN-GA). Generally, a genetic algorithm (GA) provides a huge variety of possible solutions for a certain problem; then each of the solutions is evaluated based on the fitness function.

Next, a set of the best solutions produces new solutions. Hence, the search space is driven to find the best possible solution [29, 30]. In this phase, to optimize the mapping process in the feature space, the weights are assigned to the extracted features using the GA. In our application, the solutions are the weights that have been assigned to the features. The GA finds the weights in the way that the fitness function should be minimized.

As a rule, the weights assigned to the features must satisfy two conditions. First, when the weights are assigned, the discrimination of autistic children from normal ones must be performed more accurately. Second, the weights must have a high degree of reliability and generalization. In our application, since the weights are assigned to the features to distinguish autistic children from normal ones with a minimum error, the classification error is considered the fitness function. To achieve the weights with the highest possible generalization, the K-nearest neighbors (KNN) classifier is used. This nonparametric classifier distinguishes the objects on the basis of most similar training examples existing in the feature space. Finally, the fitness function is defined as

$$Fitness\ function = A - B, \tag{6}$$

where A signifies the total number of test samples that were entered to the KNN classifier, and B signifies the number of test samples classified by the KNN classifier correctly. Table 1 briefly represents the applied topologies to assign the optimized weights to the extracted features.

Classification. Classification in our case is the process of assigning a feature vector to one of the predefined classes or categories in a manner minimizing the error of classification [31]. In the ASD detection problem, the two classes are individuals with ASD (class one) and non-ASD subjects (class two). This process is usually performed by applying classifiers on the feature vectors of two classes. The essential part of this process is to know how a classifier assigns one of the two classes to an unknown feature vector. In our research, classification is carried out by three SVMs for identification of three facial expression modes. The output of a binary SVM classifier can be computed by the following expression [32]:

$$y = \mathrm{sgn}\left(\sum_{i=1}^{N} \alpha_i y_i k(x_i, x) + b\right), \tag{7}$$

where $\{x_i, y_i\}_{i=1}^{N}$ presents the training dataset in which the input vectors are $\{ x_i \in R^d \}_{i=1}^{N}$ and the class labels $y_i \in \{-1,1\}_{i=1}^{N}$, $\alpha_i > 0$ are Lagrangian multipliers. Also, b signifies the bias, and $k(x_i, x_j)$ is the kernel SVM function. In our applications, the Gaussian RBF kernel function is used.

Data Fusion at the Decision Level. Data fusion at the decision level is an effective approach in machine learning algorithms, in which the results of classifications are combined to improve the learning performance [33, 34]. To make the data integration useful, the basic classifiers must be reliable enough, and an appropriate approach must be adopted to the integrated relevant data. In such a sense, the integration approach must compensate the shortcomings of each classifier [35]. In this stage, a decision-level data fusion is used to achieve the best possible diagnostic method. Since different facial expressions probably produce different EEG patterns, they can be used as discriminative measures to differentiate between autistic children and normal ones. So, using the fusion of these patterns, we were able to obtain all

T a b l e 1. Diagnosis Results of the Proposed Structure for Autistic and Normal Subjects before and after Weighting Optimization

Т а б л и ц я 1. Результати діагностики аутистичних та нормальних суб'єктів перед оптимізацією згідно зі значеннями ваги та після такої оптимізації

Emotion modes	Accuracy rate, % (test samples)																			
	without weighting										with weighting									
	A_3	A_4	A_5	A_6	C_7	C_8	C_9	C_{10}	C_{11}	Total	A_3	A_4	A_5	A_6	C_7	C_8	C_9	C_{10}	C_{11}	Total
sadness	96.66	83.33	100	70	100	100	100	80	43.33	**85.92**	95	83.33	98.33	73.33	100	100	100	100	48.33	**88.7**
happiness	90	96.66	96.66	63.33	100	100	100	8.33	96.66	**83.51**	96.66	98.33	91.66	80	100	95	100	50	85	**88.51**
calmness	96.66	96.66	100	28.33	100	100	100	90	98.33	**89.99**	91.66	85	98.33	43.33	100	100	100	100	100	**90.92**

information, which can be used to distinguish the two groups. One way is fusion at the decision level based on the output of classification algorithms [36, 37]. The output of different classification algorithms may be stated as one of the following three forms [38]:

Type I (abstract level) in which the classifier gives one single-class label for the specific input.

Type II (rank level) in which the classifier sorts an ordered sequence of the nominated classes in a list for each specific input so that the class with the most likely features is put at the beginning of the list.

Type III (measurement level) in which the classifier assigns a measurement value to each class; this represents the degree of confidence to belonging to a specific input to a certain class.

The type-I output includes the majority voting and Bayes methods; the type II-output includes the Borda counting method and highest-rank method, and, finally, the type-III output includes the product, maximum, minimum, and summation [37, 38]. In this study, in order to achieve the optimal decision, the integration process of output of three SVM classifiers is examined based on types I and II. First, a brief explanation of the integration language is provided, and then the applied methods are described.

Let's assume that $D = \{D_1, D_2, \ldots, D_L\}$ and $\Omega = \{\omega_1, \omega_2, \ldots, \omega_K\}$ signify the set of classifiers and the set of class labels, respectively [37, 38].

In each classifier D_i, after receiving the feature vector $x \in R^n$, the output vector is produced as follows:

$$D_i(x) = [d_{i1}(x) \quad d_{i2}(x) \ldots d_{iK}(x)]^T, \tag{8}$$

where $d_{ij}(x)$ is the value reported by the classifier. The value of $d_{ij}(x)$ depends on the type of outputs, so that in type I $d_{ij}(x) \in \{0,1\}$. In other words, if the i th classifier chooses class ω_j, then d_{ij} will be equal to 1, otherwise zero. In type II, $d_{ij}(x)$ is the integer number, and in type III, $d_{ij}(x) \in [0,1]$, which signifies the score of belonging of pattern x to the class ω_j.

The integration of classifier outputs means that, by combining the output vectors of L classifiers, the vector of pattern x to K classes is defined as

$$\begin{aligned} D(x) &= F(D_1(x), D_2(x), \ldots, D_L(x))^T = \\ &= [\mu_D^1(x) \quad \mu_D^2(x) \ldots \ldots \mu_D^K(x)] \end{aligned} \tag{9},$$

where F represents the aggregation rule. After determining this vector, the class of pattern x will correspond to the greatest entry of $D(x)$. In other words, the x pattern belongs to class ω_s if

$$\mu_D^s(x) \geq \mu_D^t(x) \ \forall t = 1,2,\ldots,K \quad , t \neq s, \tag{10}$$

The output of different classifiers may be arranged in the format of a matrix called as the Decision Profile $DP(x)$, as shown here [37].

$$DP(x) = \begin{bmatrix} d_{11}(x) & \ldots & d_{1j}(x) & \ldots & d_{1K}(x) \\ \vdots & & \vdots & & \vdots \\ d_{i1}(x) & \ldots & d_{ij}(x) & \ldots & d_{iK}(x) \\ \vdots & & \vdots & & \vdots \\ d_{Li}(x) & \ldots & d_{Lj}(x) & \ldots & d_{LK}(x) \end{bmatrix}, \tag{11}$$

where the i th row of the matrix represents the output of classifier D_i for the x, pattern, and the j th column of the matrix is the decision value of pattern x to the ω_j class provided by classifiers D_1 to D_2.

Fusion Based on Type I Output. Majority Voting. In majority voting [38, 39], the ensemble decision can be described as follows. Choose class ω_k, if

$$\sum_{i=1}^{L} d_{ik} = \max_{j=1}^{K} \sum_{i=1}^{L} d_{ij}, \tag{12}$$

Naïve Bayes Combination. This scheme assumes that the classifiers are mutually independent given a class label (conditional independence) [37]. Denote by $p(s_j)$ the probability that classifier D_j labels x in class $s_j \in \Omega$. The conditional independence allows one for the following representations:

$$p(s \mid \omega_k) = p(s_1, s_2, \ldots s_L \mid \omega_k) = \prod_{i=1}^{L} p(s_i \mid \omega_k), \tag{13}$$

Then the posterior probability needed to label x is

$$\begin{aligned} p(\omega_k \mid s) &= \frac{p(\omega_k) p(s \mid \omega_k)}{p(s)} = \\ &= \frac{p(w_k) \prod_{i=1}^{L} p(s_i \mid \omega_k)}{p(s)}, \quad k = 1,2,\ldots K. \end{aligned} \tag{14}$$

The denominator does not depend on ω_k and can be ignored; so, the support for class ω_k can be calculated as

$$\mu_k(x) \propto p(\omega_k)\prod_{i=1}^{L} p(s_i \mid \omega_k)\,, \qquad (15)$$

The practical implementation of the naive Bayes (NB) method on a Z dataset with cardinality N is explained below. For each classifier D_i, a K × K confusion matrix CM^i is calculated by applying D_i to the training dataset. The (k, s) th entry of this matrix, $cm^i_{k,s}$, is the number of elements of the dataset whose true class label is ω_k, and are assigned by D_i to class ω_s. By N_s, we denote the total number of Z elements of class ω_s. Taking $cm^i_{k,s_i}/N_k$ as an estimate of the probability $p(s_i \mid \omega_k)$, we see that Eq. (15) is equivalent to

$$\mu_k(x) \propto \frac{1}{N_k^{L-1}}\prod_{i=1}^{L} cm^i_{k,s_i}\,. \qquad (16)$$

Fusion Based on Type-III output. Class-Conscious Methods. Given $DP(x)$, the class-conscious methods [38-41] operate classwise on each column of $DP(x)$.The rules are described as follows:

Sum rule: This computes the soft class label vectors using

$$\mu_j(x) = \sum_{i=1}^{L} d_{ij} \qquad j = 1,2...K\,. \qquad (17)$$

Product rule: It computes the soft class label vectors as:

$$\mu_j(x) = \prod_{i=1}^{L} d_{ij} \qquad j = 1,2,...K. \qquad (18)$$

Min rule: computes the soft class label vectors using:

$$\mu_j(x) = \min_{i=1}^{L} d_{ij} \qquad j = 1,2,...K. \qquad (19)$$

Max rule: This computes the soft class label vectors using

$$\mu_j(x) = \max_{i=1}^{L} d_{ij} \qquad j = 1,2,...K. \qquad (20)$$

Class-Indifferent Methods. Given $DP(x)$, the class-indifferent approach uses the whole of the $DP(x)$ disregarding the classes [38]. There are two different methods, decision templates and a Dempster-Shafer combination. Due to the computational complexity of these methods, the latter were not used in this study.

RESULTS

In our proposed algorithm, two cross-validation methods were applied. In the test and training stages, the hold-out and leave-one-out (LOO) methods were used, respectively [42]. Six normal and six autistic children participated in the research. From these 12 subjects, 9 children were selected for the training phase. Also, three children (including two autistic children and one normal child) were selected randomly as test samples in order to evaluate the performance of the proposed structure. The three children selected for the test stage did not participate in the training stage and parameter setting of the algorithm. These three children were unknown to the algorithm. In this paper, the autistic and normal signals are considered positive and negative classes, respectively. Therefore, true positive (TP) and true negative (TN) samplings are defined as correctly classified autistic and normal samples, respectively. Moreover, false positive (FP) and false negative (FN) samplings are defined as incorrectly classified autistic and normal samples, respectively [43]. Based on these definitions, the accuracy rate is defined as

$$Accuracy = \frac{TP + TN}{TP + TN + FP + FN}\,. \qquad (21)$$

Autism Diagnosis Results. Finally, the proposed structure can distinguish the autistic patterns from the normal ones sufficiently accurately. To improve the process of distinguishing the autistic from normal children, the GA was used to assign the weight to the extracted features from the brain signals during processing the facial expressions. Table 2 demonstrates the overall diagnostic process of patterns in the three emotional states before and after assigning the weights to features in the training phase. Comparison of the values of Table 3 clearly reveals the improved classification performance before and after the weight assignment. In Table 2, there are two groups, autistic and control children marked with A_n and C_m, respectively, where n and m are the participant indices.

Although assigning the weight to features enhances the performance of the classification process, our goal was to achieve the highest possible accuracy of the diagnosis rate. Therefore, we apply data fusion at the decision level. Figure 4 shows the results of applying

T a b l e 2. Diagnosis Results of Autistic and Normal EEG Signals during Processing of Emotional Facial Expressions

Т а б л и ц я 2. Результати діагностики ЕЕГ-сигналів, записаних у перебігу обробки інформації щодо емоційних виразів обличчя аутистичними та нормальними дітьми

Accuracy rate (%)	Situation modes					
	sad		happy		calm	
Subjects	Autism	Control	Autism	Control	Autism	Control
Autism (1)	93.33	6.67	100	0	96.66	3.34
Autism (2)	86.66	13.34	100	0	86.66	13.34
Control (12)	0	100	6.67	93.33	0	100

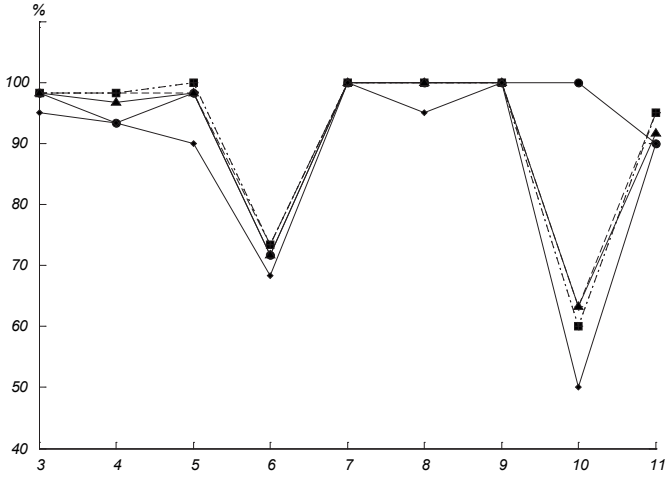

F i g. 4. Resalts of applying the fusion methods in diagnosing patterns in the training dataset.

Р и с. 4. Результати застосування методик об'єднання при діагностиці патернів у тренувальній базі даних.

different fusion methods on the outputs of classifiers. In Fig. 4, among different methods of data fusion at the decision level, the voting method demonstrated the best diagnosis performance. The voting rule at the decision level could diagnose the autistic and normal patterns at the training phase, based on the LOO assessment standard, with an accuracy rate of 94.62%.

Finally, after setting training parameters of our proposed autism diagnosis structure, a set of unknown samples was given to it, and the performance of our

T a b l e 3. Diagnosis Results of Test Patterns Based on Our Proposed Decision-Level Data-Fusion Algorithm

Т а б л и ц я 3. Результати діагностики тест-патернів, базованих на нашому запропонованому алгоритмі прийняття рішень на базі об'єднання

Test samples	Accuracy rate (%)	
	Autism	Control
Autism (1)	98.33	1.67
Autism (2)	98.33	1.67
Control (12)	0	100
Total Accuracy	98.88	

T a b l e 4. Statistical Evaluation of the Spectral Features in Some Channels

Т а б л и ц я 4. Статистична оцінка спектральних характеристик по деяких каналах

		Emotional modes		
Spectral features		sadness	happiness	calmness
MDFT	C3	1.17E-12	1.11E-19	1.90E-21
	C4	1.41E-13	1.58E-23	1.47E-13
	F3	1.13E-07	1.86E-13	2.23E-16
	F4	2.42E-13	2.31E-11	6.20E-17
	P3	1.74E-16	8.41E-28	1.12E-24
	P4	1.75E-10	2.38E-14	4.37E-11
	T3	1.90E-21	3.14E-21	8.32E-34
	T4	4.39E-22	1.06E-31	1.29E-30
Log-energy beta/alpha	C3	2.68E-14	1.19E-03	4.89E-10
	C4	1.37E-05	7.12E-01*	0.066713*
	F3	2.66E-03	8.12E-02*	8.68E-08
	F4	6.60E-09	3.36E-01*	2.03E-05
	P3	7.63E-66	2.72E-54	1.53E-53
	P4	1.32E-49	1.95E-28	3.09E-33
	T3	1.32E-54	1.24E-48	7.07E-72
	T4	1.90E-52	1.77E-24	2.53E-59
Log-energy δ		4.07E-44	5.01E-39	5.03E-34
Log-energy θ		3.88E-88	4.62E-90	1.30E-95
Log-energy α		5.26E-99	2.51E-92	4.24E-101
Log-energy β		1.50E-86	2.56E-77	2.54E-78
Log-energy γ		1.81E-66	1.89E-57	5.24E-53

* Corresponds to *P* values > 0.05; the evaluated feature is not significantly different in the two groups.

T a b l e 5. Statistical Evaluation of the Extracted MSMC Features in Two Groups for Some Channels

Т а б л и ц я 5. Статистична оцінка виділених MSMC-ознак у двох групах по деяких каналах

	Emotional modes											
	sadness				happiness				calmness			
Channel	F4	C4	T4	P4	F4	C4	T4	P4	F4	C4	T4	P4
F3	2.66E-02	2.06E-07	4.76E-07	3.21E-10	2.52E-02	9.26E-20	1.12E-12	8.24E-21	1.40E-10	1.70E-20	1.75E-16	7.34E-25
C3	3.17E-05	9.64E-10	1.00E-12	4.77E-20	3.81E-15	2.50E-20	3.49E-15	1.93E-31	1.09E-19	6.41E-22	2.65E-23	9.52E-36
T3	5.36E-06	2.31E-10	8.67E-04	3.48E-17	2.96E-12	1.81E-19	1.45E-06	6.07E-22	2.39E-17	8.22E-23	1.61E-12	2.93E-29
P3	7.71E-10	5.30E-12	1.77E-07	1.80E-12	4.91E-19	1.81E-24	1.16E-16	7.43E-32	1.47E-31	1.23E-31	1.55E-31	4.54E-35

T a b l e 6. Comparison between Our Proposed Diagnosis Structure and Those in Other Works

Т а б л и ц я 6. Порівняння успішності діагностики з використанням нашої запропонованої структури та діагностики в інших роботах

Diagnosis Algorithms	Condition	Accuracy rate (%)
Sheikhani et al. (2007) [13]	eyes open	81.0
Behnam et al. (2008) [15]	eyes open	89.5
Ahmadlou et al. (2010)[12]	resting, eyes closed	90
Razali et al. (2011) [16]	motor imitation task (to clinch their hands by following video stimuli)	86.62
Bosl et al. (2011) [17]	resting state	Control from HRA Over 80 (at age 9 months)
Shams et al. (2012) [18]	eyes open	90-100
Duffy et al. (2012) [19]	awake state	control: 88.5 ASD: 86
Alhaddad et al. (2012) [44]	relaxed condition	(91.64±.021)
Our proposed algorithm	**processing of the facial expression**	**98.88**

diagnosis structure was evaluated. Hence, EEG signals of the three children (S1, S2, and S12), which were put aside in the hold-out method, were given to our proposed structure. Table 3 shows diagnosis results of the three normal and autistic children during emotional facial expression processing. Also, Table 4 shows the final diagnosis results of the three children's brain signals by decision-level data fusion based on the voting rule.

Statistical Analysis. To evaluate the extracted features from EEG channels, the two-tailed *t*-test with a 95% confidence interval was used for the two groups (Tables 5 and 6). This statistical method was applied to the samples related to each emotional mode. Analysis of the two groups of MDFT showed significant differences for all channels and for each emotional mode. Similarly, with respect to the log-energy beta/alpha values, there were significant differences in the P3, P4, T3, and T4 electrode positions, although for the happy mode there were no differences in C4, F3, and F4 electrodes. Log-energy values in the delta, theta, alpha, beta, and gamma ranges showed the minimum *P* values, which revealed accurate estimations of the differences between ASD children and control ones. Statistical evaluation of the extracted MSMC feature in the two groups for some channels is shown in Table 6. Analysis of the MSMC values indicated significant differences between the emotional states. In other words, interhemispheric MSMC values obtained during facial expression modes can be considered a significant feature subset.

DISCUSSION

In previous researches for diagnosing the autism disorder, different techniques have been employed, and different results have been reported with respect to various test datasets. The degree of generalization and validity of a diagnosis algorithm depend on two factors, the size of the test dataset used and the type of cross-validation methods used. Recent researches in this field, with processing of EEG signals and applying different pattern recognition techniques, demonstrated prospects for EEG-based diagnosis algorithms with different performances. For example, the random sub-sampling validation technique was employed for testing the classification [12], while the k-fold validation was used to verify the results [16, 17], and the accuracy was presented by means of a LOO method [18]. As a result, due to the different databases utilized in those researches and also to different validation measures, comparing the algorithms with others in terms of accuracy is not an exact science.

Our study focused on the advantage of TOM and examined EEG signals of autistic children during processing of emotional facial expressions in three different modes. Finally, a decision-level data fusion structure based on EEG signals was proposed to diagnose autism automatically. The salient advantages of the suggested structure, as compared with other algorithms presented in the literature, include the use of a hybrid model for feature extraction, the use of an optimization algorithm to assign the weights to the extracted features, and the use of decision-level data fusion. Also, processing of different facial expressions related to the emotional state probably created different brain patterns; some of the patterns in each mode may differ between the autistic and normal children. So, using the information fusion corresponding to the three different facial expressions, we were able to achieve the greatest volume of information allowing us to distinguish the two groups from each other in each emotional mode simultaneously. Table 7 briefly illustrates a comparison between our proposed autism diagnosis structure and other algorithms presented in the literature.

Thus, a decision-level fusion-based structure using EEG signals was suggested for diagnosing autism. The EEG signals, related to three emotional facial expressions and shown by the tested children, were analyzed. In this structure, EEG signals were mapped into a vector space by applying a hybrid model. The resulting feature vectors reflect simultaneously the spatial, temporal, and spectral data, as well as the coherence degree in the distinct areas of the brain. Then, the mapping process was optimized be assigning weights to the feature using the GA. In the next stage, the features of three facial expression modes were classified. Finally, based on fusion at the decision level of three SVM classifiers, the ultimate decision was made. Thus, our technique demonstrated some advantages as compared to those proposed earlier by other authors.

Acknowledgment. The authors would like to thank Prof. A. Wahab and his research group (International Islamic University Malaysia, Kuala Lumpur, Malaysia) for making the database available for the experiments.

This study met the respective ethical principles expressed in the Helsinki Declaration (1964 and subsequent editions), which was confirmed by the Ethics Committees of the International Islamic University Malaysia (Kuala Lumpur, Malaysia) and Najafabad Branch, Islamic Azad University (Najafabad, Iran). All children were informed in detail on the testing procedure. Written informed consent was obtained from all children's parents and involved physicians.

The authors of this publication, M. Hashemian and H. Pourghassem, confirm the absence of any conflict related to the commercial or financial problems, to the relations with organizations or persons, which could in any way be associated with the investigation, and to interrelations of the co-authors.

М. Хашемян[1,2], Х. Пургассем[1,2]

СТРУКТУРА ДІАГНОСТИКИ АУТИЗМУ, БАЗОВАНА НА РІШЕННЯХ З ВИКОРИСТАННЯМ ОБ'ЄДНАННЯ ТА ІНТЕРПРЕТАЦІЇ ЕЕГ-СИГНАЛІВ, ЯКІ ПОВ'ЯЗАНІ ЗІ СПРИЙНЯТТЯМ ВИРАЗІВ ОБЛИЧЧЯ

[1] Центр цифрової обробки та дослідження зорової інформації Наджафабадського підрозділу Ісламського університету Азад (Іран).
[2] Наджафабадський підрозділ Ісламського університету Азад (Іран).

Р е з ю м е

Запропоновано структуру прийняття рішень на основі злиття при діагностиці аутизму з використанням аналізу ЕЕГ-сигналів, пов'язаних зі сприйняттям виразу обличчя. ЕЕГ-сигнали, відведені у дітей, що страждають на аутизм, і здорових дітей, записувалися під час обробки зображень емоційних виразів обличчя, таких як сум, щастя та спокій. Потім ЕЕГ-сигнали наносилися на карту простору рис. Це дозволяло сформувати нову гібридну модель, яка була організована з використанням потенціалів мозку, відведених при

вирішенні тест-завдання. Метою картування було досягти високоточного розділення аутистичних та нормальних виборок зразків. Створена карта дозволяла визначити вектори певних ознак, які відображають просторові, часові та спектральні дані, а також рівень когерентності сигналів у різних зонах мозку. Процедура картування оптимізувалася з використанням генетичного алгоритму через надання певних рівнів ваги векторам ознак. Потім вектори ознак, що відповідали трьом емоційним виразам обличчя, класифікувалися із застосуванням машин опорних векторів. Нарешті, використання рішення на основі об'єднання (згідно з правилом «голосування більшості») робило запропоновану структуру діагностики здатною ефективно розрізняти аутистичних та нормальних суб'єктів.

REFERENCES

1. American Psychiatric Association, *Diagnostic and Statistical Manual of Mental Disorders* (Fourth ed.), Am. Psychiat. Ass., USA (2000).
2. J. L. Matson and J. A. Boisijoli, "Strategies for assessing Asperger's syndrome: A critical review of data based methods," *Res. Autism Spectrum Disord*., **2**, No. 2, 237-248 (2008).
3. J. L. Matson and N. F. Minshawi, *Early Intervention for Autism Spectrum Disorders: A Critical Analysis*, Elsevier Sci. Inc, Oxford (2006).
4. S. Baron-Cohen, F. J. Scott, C. Allison, et al., "Prevalence of autism-spectrum conditions: UK school-based population study," *Brit. J. Psychiat*., **194**, No. 6, 500-509 (2009).
5. T. S. Brugha, S. McManus, J. Bankart, et al., "Epidemiology of autism spectrum disorders in adults in the community in England," *Arch. Gen. Psychiat*., **68**, No. 5, 459-465 (2011).
6. C. Rice, "Prevalence of autism spectrum disorders - Autism and developmental disabilities monitoring network, United States," *MMWR Surveill Summ*., **58**, 1-20 (2009).
7. E. Fombonne, "Epidemiology of pervasive developmental disorders," *Pediat. Res*., **65**, No. 6, 591-598 (2009).
8. A. Ghanizadeh, "A preliminary study on screening prevalence of pervasive developmental disorder in school children in Iran," *J. Autism Dev. Disord*., **38**, No. 4, 759-763 (2008).
9. A. Nejatisafa, M. R. Kazemi, and J. Alaghebandrad, "Autistic features in adult population: evidence for continuity of autistic symptoms with normality," *Adv. Cogn. Sci*., **5**, No. 3, 34-39 (2003).
10. M. Othman and A. Wahab, "Affective face processing analysis in autism using electroencephalogram," in: *3rd Int. Conf. Inform. Commun. Technol. Muslim World (ICT4M)*, *Jakarta, Dec. 3-4* (2010), pp. E23-E27.
11. M. Hashemian and H. Pourghassem, "Facial emotion processing in autism spectrum disorder based on spectral features of EEG signals," *Int. J. Imag. Robotics*, **11**, No. 3, 68-80 (2013).
12. M. Ahmadlou, H. Adeli, and A. Adeli, "Fractality and a wavelet-chaos-neural network methodology for EEG-based diagnosis of autistic spectrum disorder," *J. Clin. Neurophysiol*., **27**, No. 5, 328-333 (2010).
13. M. Hashemian and H. Pourghassem, "Autism spectrum disorders analysis based on EEG signal: a survey," *Neurophysiology*, **46**, No. 2, 183-195 (2014).
14. A. Sheikhani, H. Behnam, M. Mohammadi, and M. Noroozian, "Analysis of quantitative electroencephalogram background activity in autism disease patients with Lempel-Ziv complexity and short time fourier transform measure," in: *Proc. 4th IEEE-EMBS*, Cambridge (2007), pp. 19-22.
15. H. Behnam, A. Sheikhani, M. R. Mohammadi, et al., "Abnormalities in connectivity of quantitative electroencephalogram background activity in autism disorders especially in left hemisphere and right temporal," in: *Proc. 10th Int. Conf. Computer Model. Simul., 1-3 April* (2008).
16. N. Razali and A. Wahab, "2D Affective Space Model (ASM) for detecting autistic children," in: *Proc. 15th IEEE Int. Sympos. Consumer Electron*., Singapore (2011), pp. 536-541.
17. W. Bosl, A. Tierney, H. Tager-Flusberg, and C. Nelson, "EEG complexity as a biomarker for autism spectrum disorder risk," *BMC Med.*, **9**, No. 18 (2011).
18. W. Khazal Shams and A. Wahab, "Characterizing autistic disorder based on principal component analysis," *Austral. J. Basic Appl. Sci*., **6**, No. 1, 149-155 (2012).
19. F. H. Duffy and H. Als, "A stable pattern of EEG spectral coherence distinguishes children with autism from neurotypical controls - a large case control study," *BMC Med.*, **10**, No. 64 (2012).
20. M. Behnam and H. Pourghassem, "Real-time seizure prediction using rls filtering and interpolated histogram feature based on hybrid optimization algorithm of bayesian classifier and hunting search," *Comput. Methods Prog. Biomed.*, **132**, No. 8, 115-136 (2016).
21. S. Nasehi and H. Pourghassem, "Mental task classification based on HMM and BPNN," in" *Proc. Int. Conf. Commun. Systems Network Technol.* (CSNT 2013), *Gwalior, India, 6-8 Apr*. (2013), pp. 210-214.
22. M. Behnam and H. Pourghassem, "Seizure-specific wavelet (seizlet) design for epileptic seizure detection using correntropy ellipse features based on seizure modulus maximas patterns," *J. Neurosci. Methods*, **276**, No. 2, 84-107 (2017).
23. H. Adeli, S. Ghosh-Dastidar, and N. Dadmehr, "A wavelet-chaos methodology for analysis of EEGs and EEG subbands to detect seizure and epilepsy," *IEEE Trans. Biomed. Engineer.,* **54**, No. 2, 205-211 (2007).
24. S. Nasehi and H. Pourghassem, "A novel fast epileptic seizure onset detection algorithm using general tensor discriminant analysis," *J. Clin. Neurophysiol*., **30**, No. 4, 362-370 (2013).
25. S. Nasehi and H. Pourghassem, "Online mental task classification based on DWT-PCA features and probabilistic neural network," *Int. J. Imag. Robotics*, **7**, No. 1, 110-118 (2012).
26. B. Danny Oude, "EEG-based emotion recognition. The influence of visual and auditory stimuli," *Emotion*, **57**, No. 7, 1798-1806 (2006).
27. P. L. Nunez, R. Srinivasan, A. F. Westdorp, et al., "EEG coherency. I. Statistics, reference electrode, volume conduction, Laplacians, cortical imaging, and interpretation at multiple scales," *Electroencephalogr. Clin. Neurophysiol*., **103**, No. 5, 499-515 (1997).
28. R. Srinivasan, P. L. Nunez, and R. B. Silberstein, "Spatial filtering and neocortical dynamics: Estimates of EEG coherence," *IEEE Trans. Biomed. Engineer.*, **45**, No. 7, 814-826 (1998).
29. H. Pourghassem and S. Daneshvar, "A framework for medical image retrieval using merging-based classification with dependency probability-based relevance feedback," *Turk. J. Electr. Eng.. Comput. Sci.*, **21**, No. 3, 882-896 (2013).

30. M. Nurmohamadi and H. Pourghassem, "Clavulanic acid production estimation based on color and structural features of *Streptomyces clavuligerus* bacteria using self-organizing map and genetic algorithm," *Comput. Methods Prog. Biomed.*, **114**, No. 3, 337-348 (2014).
31. S. Nasehi and H. Pourghassem, "Seizure detection algorithms based on analysis of EEG and ECG signals: A survey," *Neurophysiology*, **44**, No. 2, 174-186 (2012).
32. S. M. Zhou, J. Q. Gan, and F. Sepulveda, "Classifying mental tasks based on features of higher-order statistics from EEG signals in brain–computer interface," *Inform. Sci.*, **178**, 1629-1640 (2008).
33. M. Behnam and H. Pourghassem, "Optimal query-based relevance feedback in medical image retrieval using score fusion-based classification," *J. Digital Imag.*, **28**, No. 2, 160-178 (2015).
34. S. Momeni and H. Pourghassem, "An automatic fuzzy-based multi-temporal brain digital subtraction angiography image fusion algorithm using curvelet transform and content selection strategy," *J. Med. Syst.*, **38**, No. 8, 1-16 (2014).
35. R. Rastghalam and H. Pourghassem, "Breast cancer detection using MRF-based probable texture feature and decision-level fusion-based classification using HMM on thermography images," *Pattern Recogn.*, **51**, No. 3, 176-186 (2016).
36. L. Xu, A. Krzyzak, and C. Y. Suen, "Methods of combining multiple classifiers and their applications to handwriting recognition," *IEEE Trans. Syst., Man, Cybern.*, **22**, 418-435 (1992).
37. L. I. Kuncheva, *Combining Pattern Classifiers: Methods and Algorithms*, Wiley Interscience (2004).
38. L. Lam and C. Y. Suen, "Optimal combinations of pattern classifiers," *Pattern Recogn. Lett.*, **16**, 945-954 (1995).
39. U. G. Mangai, S. Samanta, S. Das, and P. R. Chowdhury, "A survey of decision fusion and feature fusion strategies for pattern classification," *IETE Tech. Rev.*, **27**, 293-307 (2010).
40. J. V. Kittler, M. Hatef, R. P. W. Duin, and J. Matas, "On combining classifiers," *IEEE Trans. Pattern Anal. Mach. Intelligence*, **20**, No. 3, 226-239 (1998).
41. L. Lam and C. Y. Suen, "Optimal combinations of pattern classifiers," *Pattern Recogn. Lett.*, **16**, Nos. 1/3, 945-954 (1995).
42. A. Tahmasebi and H. Pourghassem, "A novel intra-class distance-based signature identification algorithm using weighted gabor features and dynamic characteristics," *Arab. J. Sci. Eng.*., **38**, No. 11, 3019-3029 (2013).
43. M. Behnam and H. Pourghassem, "Periodogram pattern feature-based seizure detection algorithm using optimized hybrid model of MLP and ant colony," in: *Proc. 23rd Iranian Conf. Electrical Engineer. (ICEE 2015)*, *Tehran, Iran, May* (2015), pp. 32-37.
44. M. J. Alhaddad, M. I. Kamel, H. M. Malibary, et al., "Diagnosis of autism by Fisher linear discriminant analysis FLDA via EEG," *Int. J. Biosci. Biotechnol.*, **4**, No. 2, 45-54 (2012).